

# Nanoscale

Accepted Manuscript



This is an *Accepted Manuscript*, which has been through the Royal Society of Chemistry peer review process and has been accepted for publication.

*Accepted Manuscripts* are published online shortly after acceptance, before technical editing, formatting and proof reading. Using this free service, authors can make their results available to the community, in citable form, before we publish the edited article. We will replace this *Accepted Manuscript* with the edited and formatted *Advance Article* as soon as it is available.

You can find more information about *Accepted Manuscripts* in the [Information for Authors](#).

Please note that technical editing may introduce minor changes to the text and/or graphics, which may alter content. The journal's standard [Terms & Conditions](#) and the [Ethical guidelines](#) still apply. In no event shall the Royal Society of Chemistry be held responsible for any errors or omissions in this *Accepted Manuscript* or any consequences arising from the use of any information it contains.

## Controlled Synthesis and Assembly into Anisotropy Arrays of Magnetic Cobalt-Substituted Magnetite Nanocubes

Weiwei Yang,<sup>1</sup> Yongsheng Yu,<sup>1\*</sup> Liang Wang,<sup>2</sup> Chunhui Yang,<sup>1</sup> and Haibo Li<sup>3</sup>

<sup>1</sup>School of Chemical Engineering and Technology, Harbin Institute of Technology, Harbin, Heilongjiang 150001, China

<sup>2</sup>School of Materials Science and Engineering, Harbin Institute of Technology, Harbin 150001, China

<sup>3</sup>Key Laboratory of Functional Materials Physics and Chemistry of the Ministry of Education, Jilin Normal University, Changchun 130103, China

E-mail: ysyu@hit.edu.cn

---

**Abstract** Cube cobalt-substituted magnetite  $\text{Co}_x\text{Fe}_{3-x}\text{O}_4$  nanocubes (NCs) with the uniform composition distributions of Co, Fe and O in the NCs through solution synthesis were reported in this paper. Through controlling reaction conditions, the size of the cube NCs could be tuned from 35 to 110 nm. It was found that the cube shape could easily induce the (400) orientation of the NCs on the Si substrate and applying the external magnetic field in out-of-plane direction could further enhance the (400) orientation of these NCs on Si substrate. The highest 2.07 kOe coercivity could be obtained by assembling the NCs in the external magnetic field. The reported magnetic cobalt-substituted magnetite NCs provide an ideal class of building blocks for studying ferrimagnetic nanoparticle (NP) assembly with easily controlled magnetic alignment for magnetic tape recording with ever increased areal storage density.

---

Synthesis of ferromagnetic (FM) or ferrimagnetic (FIM) NP with controlled morphology has attracted significant attention to future fabrication of magnetic NP arrays with controlled magnetization directions for many technological applications including data and energy storage applications.<sup>1-9</sup> Usually, FM NPs with very high magnetocrystalline anisotropy, especially tetragonal FePt,<sup>10,11</sup> NdFeB,<sup>12</sup> and hexagonal SmCo<sup>13</sup> based alloy NPs, can hold their magnetic moments in some direction and be used as building blocks for permanent magnets and for studying nanomagnetism. However, monodisperse FePt NPs prepared from solution phase syntheses tend to be superparamagnetic. In order to obtain monodisperse hard magnetic FePt NPs with high magnetocrystalline anisotropy, one can coat the as-synthesized FePt NPs with SiO<sub>2</sub> before thermal annealing, and remove SiO<sub>2</sub> layer by base washing after the faced-center tetragonal (fct) FePt phase is formed.<sup>14-17</sup> Alternatively, the as-synthesized FePt NPs can be ground with a large excess of NaCl before thermal annealing, and NaCl can be dissolved with water.<sup>18</sup> Despite these efforts, stabilizing a FM FePt NP dispersion is still challenging. Rare-earth metal based alloy NPs of SmCo and NdFeB are extremely difficult to prepare and stabilize

due to the easy oxidation of Sm(0) and Nd(0) in the alloy structures. Furthermore, rare-earth elements are increasingly rare and expensive, and alternative permanent magnet materials which do not contain rare-earth and noble metal elements are needed by the industry.<sup>19,20</sup> The magnetocrystalline anisotropic constant of Co-substituted Fe<sub>3</sub>O<sub>4</sub> (Co<sub>x</sub>Fe<sub>3-x</sub>O<sub>4</sub>, 0 < x ≤ 1) can reach as high as 5 × 10<sup>5</sup> J/m<sup>3</sup>, which means that Co<sub>x</sub>Fe<sub>3-x</sub>O<sub>4</sub> could provide a more accessible NP system than any of the FePt, SmCo and NdFeB for NP magnetism studies.<sup>21-27</sup>

Co-substituted Fe<sub>3</sub>O<sub>4</sub> NPs were traditionally synthesized by coprecipitation of Co- and Fe-salts.<sup>28-31</sup> However, FIM NPs prepared from these methods do not have the desired controls on sizes and morphologies. Recently, we demonstrated that monodisperse cobalt-substituted magnetite Co<sub>x</sub>Fe<sub>3-x</sub>O<sub>4</sub> NPs with high coercivity could be synthesized by solution phase syntheses. The highest 1.69 kOe coercivity of the as-synthesized randomly oriented NPs could be obtained.<sup>32</sup> However, these NPs have polyhedral morphology. In order to obtain high magnetic energy production or areal storage density, the permanent magnets composed of hard magnetic NPs should have high packing density. For the optimized magnetic applications, cube shaped NPs should orient into arrays with 100% packing density. In addition, as the magnetic easy axis of a NP correlates closely with its crystal structure, the shape induced crystal orientation of each NP in an assembly would lead to an aligned magnetic easy axis. Such alignment is often a necessity for a NP assembly to be suitable for various magnetic applications in such as data storage and permanent magnets. For the NCs, the crystal orientations of each NCs are easy to align in the same direction, which means that high packing density and easy axis alignment could be easily achieved by NCs assembly. However, magnetic NCs were only achieved in several systems, such as Fe<sub>3</sub>O<sub>4</sub>,<sup>33-36</sup> Ni,<sup>37</sup> FePt,<sup>37</sup> Co(Ni)Pt,<sup>39</sup> Wüstite-Spinel Core-Shell NPs,<sup>40</sup> MnZn ferrite NPs<sup>41</sup>. Actually, the synthesis conditions should be carefully controlled to form NCs compared to round or polyhedral due to the higher energy of the (100) planes compared to (111) planes in nano-size. Right now, hard magnetic NCs with size control directly from solution phase syntheses have not been reported.

Herein, we report a simple synthesis of hard magnetic cobalt-substituted magnetite Co<sub>x</sub>Fe<sub>3-x</sub>O<sub>4</sub> NCs by modifying the recipe reported by D. Kim *et al.*<sup>32</sup> In this improved synthesis, Co(acac)<sub>2</sub> and Fe(acac)<sub>3</sub> were dissolved in benzyl ether (BE) in the presence of oleic acid (OA) (see the **Supporting Information**). The size of NCs was controlled by the amounts of OA and BE. For example, to make 50 nm Co<sub>0.4</sub>Fe<sub>2.6</sub>O<sub>4</sub> NCs, Fe(acac)<sub>3</sub> (1.330 mmol), Co(acac)<sub>2</sub> (0.665 mmol), OA (2.5 mL) and BE (20 mL) were mixed and stirred under nitrogen. The solution was directly heated to 290 °C at the rate 20 °C/min and maintained at this temperature for 30 min before it was cooled down to room temperature. The product was separated and redispersed in hexane.

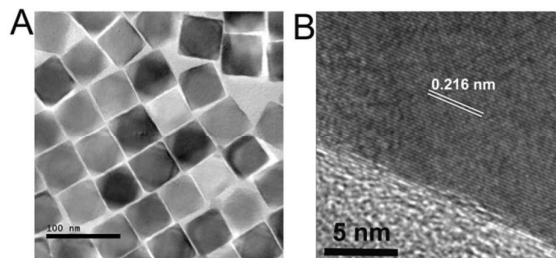


**Figure 1.** (A) TEM image of the 50 nm  $\text{Co}_{0.4}\text{Fe}_{2.6}\text{O}_4$  NCs synthesized at 290 °C for 30 min with a heating rate of 20 °C/min and (B) HRTEM image of a representative NC shown in (A).

To achieve a shape-controlled synthesis, it is important to control the growth rate along specific direction and the nucleation during the initial stage of the reaction. Hence, in the synthesis, we first studied heating rate on the NP morphology and composition controls. And the heating rates of 2.5, 10 and 20 °C/min were used in the synthesis. Transmission electron microscopy (TEM) analysis showed that both size and morphology of the NPs separated from different heating rates were nearly the same. **Figure 1A** shows a typical TEM image of the  $\text{Co}_{0.4}\text{Fe}_{2.6}\text{O}_4$  NCs with their size being at  $50 \pm 5$  nm synthesized at 290 °C for 30 min with a heating rate of 20 °C/min. **Figure 1B** shows the HRTEM image of a representative NC from Figure 1A. The NC is in single crystalline and has a lattice fringe of 0.216 nm, close to the spacing of the (400) planes in inverse spinel structured face centered cubic (fcc)  $\text{CoFe}_2\text{O}_4$  (0.21 nm). It could be clearly seen that the (400) planes in the HRTEM image are parallel with the surface of the NC, which means that the surface planes of the NC are (400) planes. The crystal structure of the NCs was further characterized by X-ray diffraction (XRD) (**Figure S1**). The XRD patterns show the typical (311), (400), (511), and (440) diffraction peaks of the fcc structure, which means that  $\text{Co}_{0.4}\text{Fe}_{2.6}\text{O}_4$  NCs with the inverse spinel structure could be easily synthesized by simply heating the solution to the reaction temperature.

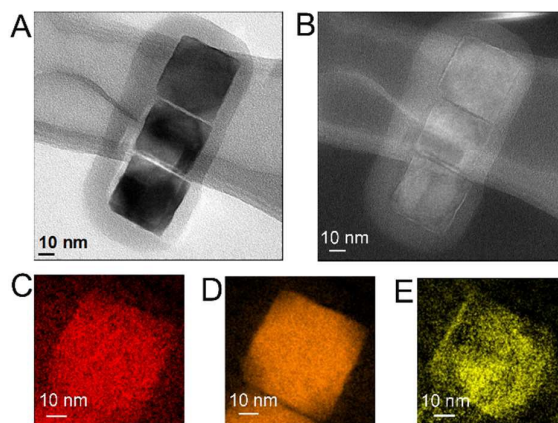


**Figure 2.** (A) the thickness mapping and (B) the zero loss map of the 50 nm  $\text{Co}_{0.4}\text{Fe}_{2.6}\text{O}_4$  NCs synthesized at 290 °C for 30 min with a heating rate of 20 °C/min. and the elemental mappings of O (C), Fe (D) and Co (E) in each NP shown in (B)

Due to fast heat to the reaction temperature, the nucleation of the NCs and the growth of the nuclei would happen at the same time, which means that it is worthy to further research the shape of the as-synthesized NCs. And **Figure 2A** shows the typical thickness mapping of the 50 nm  $\text{Co}_{0.4}\text{Fe}_{2.6}\text{O}_4$  NCs synthesized at 290 °C for 30 min with a heating rate of 20 °C/min, which indicates that the distribution and variation of the thickness for the NCs. Compared with the zero loss map which is the image reconstruction from the signals of the zero loss peak from electron energy-loss spectroscopy (EELS) shown in **Figure 2B**, it is further confirmed that the as-synthesized NPs have the cube shape. In the current synthesis, the ratio of  $\text{Co}(\text{acac})_2/\text{Fe}(\text{acac})_3$  is fixed at 1:2. The ratio of Co/Fe in the NPs 1:6.5, which is lower than the ratio of initial metal precursors. Slowly heating the solution to the reaction temperature led to more Co(II) replacement of the Fe(II) in the inverse spinel structure. For the heating rates of 2.5 and 10 °C/min,  $\text{Co}_{0.5}\text{Fe}_{2.5}\text{O}_4$  NPs could be obtained, suggesting that Co(II) did not replace all of the Fe(II) in the inverse spinel structure, even for slowly heating rate. In order to obtain the high magnetocrystalline anisotropic constant for cobalt-substituted magnetite, cobalt-substituted magnetite should have the uniform composition distributions in the NCs. And the composition distributions in the as-synthesized NCs were further characterized by the atomically resolved aberration-corrected scanning transmission electron microscopy-EELS (STEM-EELS). And one typical NC in **Figure 2B** was compositionally analyzed. **Figure 2C-E** show the elemental mappings of O (red), Fe (brown) and Co (yellow) in the NC. The color distribution within the NC indicates that all three elements have the uniform composition distributions in the NC and the cobalt-substituted magnetite alloy structure is formed indeed in the NC. These results suggest that the cube cobalt-substituted magnetite with the uniform composition distribution could be obtained by fast heating the solution to the reaction temperature.

Previous in order to synthesize  $\text{MFe}_2\text{O}_4$  (M = Fe, Co, Mn) NPs with the uniform composition distribution in NPs, the solution should be first heated to 200 °C and remained at that temperature for some time before it is heated to reflux at 290 °C.<sup>42</sup> In the current synthesis, we found that if the solution was maintained at 200 °C for 30 min and then fast heated to 290 °C with a heating rate of 20 °C/min, the  $35\pm 5$  nm  $\text{Co}_{0.4}\text{Fe}_{2.6}\text{O}_4$  with polyhedral shape could be obtained, as shown in **Figure S2**. This result suggests that maintaining at 200 °C for 30 min might produce more the nucleation of the NPs, which would grow to the smaller NPs than those shown in **Figure 1A**. And increasing the nucleation time would lead to the isotropy growths of the  $\text{Co}_{0.4}\text{Fe}_{2.6}\text{O}_4$  crystal planes to lower the surface energy of the NPs, which would produce the polyhedral shape. In the NCs synthesis, the process of maintaining at 200 °C for 30 min was deleted during the synthesis. And the solution was directly heated to the reflux temperature, which led to the fast anisotropic growth of the NPs, producing the NCs with the (400) planes with the higher energy on the surface.

Oleylamine (OAm) as both reducing agent and surfactant is usually used in the synthesis of transition metal oxide NPs.<sup>34, 42</sup> By changing the amount of OAm used in the synthesis, the size, morphology and composition of the NPs could be easily tuned. In the current synthesis, we also found that the size and shape of the as-synthesized

NPs were strongly influenced by small additions of OAm. In a series of experiments, the amount of OA was kept constant at 2.5 mL. And 1.330 mmol  $\text{Fe}(\text{acac})_3$  and 0.665 mmol  $\text{Co}(\text{acac})_2$  were used in the synthesis. With the addition of 0.5 mL OAm, the monodisperse NCs could be still obtained, as shown in **Figure S3A**. Compared with **Figure 1A**, the size of the NCs decreases to  $38 \pm 3$  nm. With increasing the amount of OAm to 1.0 mL, around 20 nm cube-like NPs (**Figure S3B**) could be observed beside some 35 nm cube NPs in the production. When the amount of OAm was further increased to 2.0 mL, most NPs shown in **Figure S3C** have irregular shape. Base on these results, we can see that OA with a carboxylic group,  $-\text{COOH}$ , has a selective binding onto higher energy crystal planes, which could facilitate the formation of the NCs. And OAm with a  $-\text{NH}_2$  group has a weak and isotropic binding onto the surface planes of the NPs, which easily promotes the formation of the round or polyhedral shape NPs.

The size and morphology of the as-synthesized NCs could be further controlled by the amounts of OA and BE present in the reaction mixture heated at  $290^\circ\text{C}$ . More OA (3.1 mL) in the reaction mixture gave smaller ( $35 \pm 4$  nm)  $\text{Co}_{0.4}\text{Fe}_{2.6}\text{O}_4$  NCs (**Figure 3A**). Decreasing the amount of OA produced bigger NCs. 1.27 mL OA used in the reaction yielded  $\text{Co}_{0.5}\text{Fe}_{2.5}\text{O}_4$  NCs with size at  $65 \pm 4$  nm (**Figure 3B**). We found that further decreasing the amount of OA could not produce the much bigger cube NPs. When 0.9 mL OA was used in the reaction, the mixture of cube and irregularly shaped NPs could be obtained (**Figure 3C**), which means that less OA could not facilitate NP growth along  $\langle 400 \rangle$  directions into NCs or to grow the much bigger NCs. When 10 mL BE and 1.27 mL OA were used in the reaction, which means increasing the concentrations of the precursors in the reaction, concave-cube-like  $\text{Co}_{0.5}\text{Fe}_{2.5}\text{O}_4$  NPs with size at  $110 \pm 10$  nm could be obtained (**Figure 3D**). These samples have the similar XRD patterns and show the inverse spinel structure (**Figure S4**). These results suggest that the amounts of OAc and BE could be effective to tune the sizes of cobalt-substituted magnetite NCs.

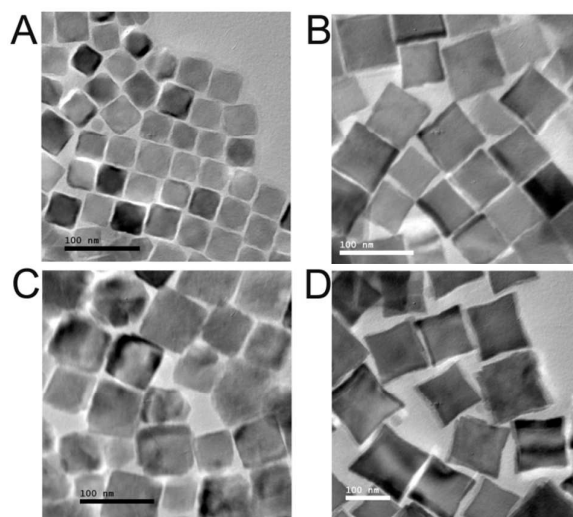


**Figure 3.** TEM images of the as-synthesized  $\text{Co}_x\text{Fe}_{3-x}\text{O}_4$  NCs with OA (A) 3.1 mL, (B) 1.27 mL, (C) 0.9 mL, and (D) 10 mL BE and 1.27 mL OA.

Magnetic properties of the 50 nm NCs synthesized at 290 °C from different heating rates were measured by a vibrating sample magnetometer (VSM) with fields up to 12.5 kOe at room temperature, as shown in **Figure 4A**. The  $\text{Co}_{0.4}\text{Fe}_{2.6}\text{O}_4$  NCs prepared from the heating rate of 20 °C/min have an  $H_c$  of 1.29 kOe and an  $M_s$  of 85.4 emu/g. In comparison,  $H_c$  of the  $\text{Co}_{0.5}\text{Fe}_{2.5}\text{O}_4$  NCs from the heating rate of 2.5 °C/min decreases to 1.00 kOe, while their  $M_s$  increases to 89.9 emu/g. In the current synthesis, all the as-synthesized cobalt-substituted magnetite NCs have the inverse spinel structure, which means that Fe(III) ions were reduced in to Fe(II) in the reaction. It is thought that cobalt-substituted magnetite NCs were obtained through the thermal decomposition reaction of iron-oleate and cobalt-oleate complex which were acquired by the reaction of  $\text{Fe}(\text{acac})_3$  and  $\text{Co}(\text{acac})_2$  with OA, during the reaction. And the thermal decompositions of these metal-oleate complexes could produce CO,  $\text{H}_2$ , and carbon, which are responsible for the reduction of Fe(III) to Fe(II).<sup>43</sup> The coercivity decrease and moment increase with lower heating rate might be caused likely by the reduction of Fe(III) to Fe(II) by CO,  $\text{H}_2$ , and carbon, eliminating partially the antiferromagnetic coupling between two Fe(III) ions in the inverse spinel structure, which led to the increase of  $M_s$ . Since the cobalt-substituted magnetite NCs with different size in the current synthesis shows the similar composition, the size dependent magnetic properties of cobalt-substituted magnetite NCs synthesized at 290 °C for were summarized in **Figure 4B**. It could be seen that 35 nm NCs have the highest  $H_c$  of 1.48 kOe and the coercivities of the NCs decrease with increasing the size of NCs. This result is similar with those reported in some literates.<sup>44, 45</sup> The decrease of  $H_c$  in the current research might be attributed to the transformation from the single domain to the multi domain in the NCs with increasing the size of NCs. The remanence ratios also decrease with increasing the size of the NCs, which might have a contribution from the development of domain walls in the NCs.<sup>44</sup>

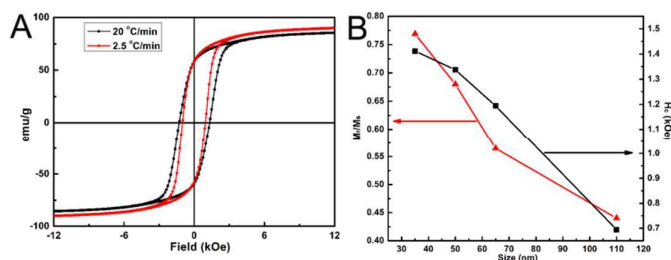


**Figure 4.** (A) Hysteresis loops of the  $\text{Co}_x\text{Fe}_{3-x}\text{O}_4$  NCs prepared from the heating rate of 2.5 and 20 °C/min. (B) The size dependent magnetic properties of cobalt-substituted magnetite NCs synthesized at 290 °C with the heating rate of 20 °C/min.

To investigate possible preferential orientation in the arrangement of the NCs on Si substrate, the 50 nm NCs synthesized at 290 °C for 30 min with a heating rate of 20 °C/min were loaded on Si substrate by controlled evaporation of the carrier solvent from the hexane dispersion. Scanning electron microscopy (SEM) image of the NCs on Si substrate (**Figure 5A**) shows the surface planes of most NCs are paralleled with

the surface of the substrate, indicating the (400) orientation of the NCs. Since  $\langle 100 \rangle$  direction of cobalt-substituted magnetite is the easy axis, it is possible to further enhance (400) orientation by applying external magnetic field in out-of-plane direction. The 50 nm cube NC dispersion was also dropped on Si substrate under a magnet ( $H = 5.5$  kOe) perpendicular to the surface of the Si substrate. Compared with **Figure 5A**, the NCs assembled on Si substrate in the external magnetic field (**Figure 5B**) show the more uniform morphology and the (400) planes of almost all the NCs are paralleled with the surface of the substrate. In order to further confirm the (400) orientation of the NCs on Si substrate, these two samples were also measured by  $\theta$ - $2\theta$  scan of XRD. XRD pattern of the NCs on Si substrate shows a strongest (400) peak (**Figure 5C**). This is markedly different from that of a 3D randomly oriented 50 nm NCs with a strongest (311) peak (as shown in **Figure S1**), further indicating that each NC on Si substrate has a preferred crystal orientation with (400) planes parallel to the substrate. It could be seen that the relative intensity of (400) peak further increases and the relative intensity of (311) peak decreases when the NCs were assembled on Si substrate in the external magnetic field. And the intensity ratio of  $I_{(400)} / I_{(311)}$  increases from 1.9 for the NCs on Si substrate without applying external magnetic field to 3.9 for the NPs on Si substrate with external magnetic field alignment. These results suggest that the cube shape is easy to induce the (400) orientation of the NCs and applying the external magnetic field in out-of-plane direction could further enhance the (400) orientation of these NCs on Si substrate. The magnetic properties of the NCs on Si substrate without (and with) external magnetic field alignment were shown in **Figure 5D&E**. It could be clear seen that both samples have the perpendicular anisotropy. The coercivity increases from 1.49 kOe for the NCs on Si substrate without applying external magnetic field to 2.07 kOe for the NCs on Si substrate with external magnetic field alignment, which also confirms that applying the external magnetic field in out-of-plane direction could further enhance the perpendicular anisotropy of the NCs on Si substrate.

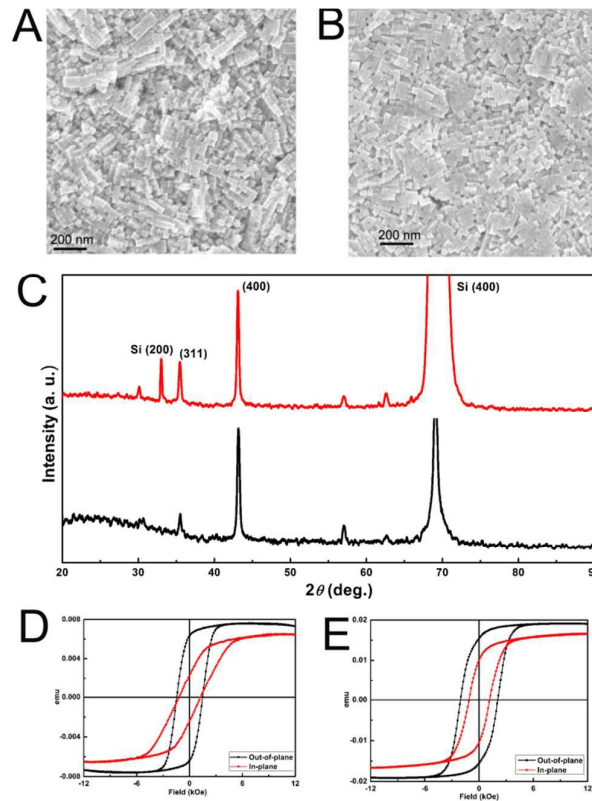


**Figure 5.** SEM images of the 50 nm NCs assembled on Si substrate without (A) and with (B) external magnetic field alignment. (C) XRD patterns of the NCs on Si substrate without (red curve) and with (black curve) external magnetic field alignment. Hysteresis loops of the NCs on Si substrate without (D) and with (E) external magnetic field alignment.

We have reported a simple process to prepare monodisperse cobalt-substituted magnetite  $\text{Co}_x\text{Fe}_{3-x}\text{O}_4$  NCs with the uniform composition distributions of Co and Fe in the NCs through solution synthesis in the presence of oleic acid as surfactant. Through controlling reaction conditions, the size of the cube NCs could be tuned from 35 to 110 nm. We also demonstrated that the cube shape could easily induce the (400) orientation of the NCs on the Si substrate and applying the external magnetic field (5.5 kOe) in out-of-plane direction could further enhance the (400) orientation of these NCs on Si substrate. When assembled under an external magnetic field, these NCs show the preferred magnetic alignment with their  $H_c$  reaching 2.07 kOe. The reported cobalt-substituted magnetite NCs provide an ideal class of building blocks for studying ferrimagnetic NP assembly with controlled magnetic alignment for magnetic tape recording with ever increased areal storage density.

**ACKNOWLEDGMENTS.** This work was supported by the National Natural Science Foundation of China under Grant (No. 51101069, 21305025, and 21371071).

## REFERENCES

- (1) H. Zeng, J. Li, J. P. Liu, Z. L. Wang, S. H. Sun, *Nature*, 2002, 420, 395-398.

- (2) J. Park, K. An, Y. Hwang, J. G. Park, H. J. Noh, J. Y. Kim, J. H. Park, N. M. Hwang, and T. Hyeon, *Nat. Mat.* 2004, 3, 891-895.
- (3) S. H. Sun, *Adv. Mater.* 2006, 18, 393-403.
- (4) N. Sakuma, T. Ohshima, T. Shoji, Y. Suzuki, R. Sato, A. Wachi, A. Kato, Y. Kawai, A. Manabe, and T. Teranishi, *ACS Nano*, 2011, 5, 2806-2814.
- (5) B. Balasubramanian, R. Skomski, X. Z. Li, S. R. Valloppilly, J. E. Shield, G. C. Hadjipanayis, and D. J. Sellmyer, *Nano Lett.* 2011, 11, 1747-1752.
- (6) H. W. Zhang, S. Peng, C. B. Rong, J. P. Liu, Y. Zhang, M. J. Kramer and S. H. Sun, *J. Mater. Chem.* 2011, 21, 16873-16876.
- (7) X. Q. Liu, S. H. He, J. M. Qiu, and J. P. Wang, *Appl. Phys. Lett.* 2011, 98, 222507-222509.
- (8) B. Balamurugan, B. Das, V. R. Shah, R. Skomski, X. Z. Li, and D. J. Sellmyer, *Appl. Phys. Lett.* 2012, 101, 122407-122409.
- (9) L. J. Zhu, S. H. Nie, K. K. Meng, D. Pan, J. H. Zhao, and H. Z. Zheng, *Adv. Mater.* 2012, 24, 4547-4551.
- (10) J. Kim, C. B. Rong, J. P. Liu, and S. H. Sun, *Adv. Mater.* 2009, 21, 906-909.
- (11) J.-M. Qiu, J.-P. Wang, *Adv. Mater.* 2006, 19, 1703-1706.
- (12) W. B. Cui, Y. K. Takahashi, and K. Hono, *Adv. Mater.* 2012, 24, 6530-6541.
- (13) Y. L. Hou, Z. C. Xu, S. Peng, C. B. Rong, J. P. Liu, and S. H. Sun, *Adv. Mater.* 2007, 19, 3349-3352.
- (14) S. Yamamoto, Y. Morimoto, T. Ono, M. Takano, *Appl. Phys. Lett.* 2005, 87, 032503-032505.
- (15) S. Yamamoto, Y. Morimoto, Y. Tamada, Y. K. Takahashi, K. Hono, T. Ono, M. Takano, *Chem. Mater.* 2006, 18, 5385-5388.
- (16) Y. Tamada, Y. Morimoto, S. Yamamoto, M. Takano, S. Nasu, T. Ono, *J. Magn. Magn. Mater.* 2007, 310, 2381-2383.
- (17) Y. Tamada, S. Yamamoto, M. Takano, S. Nasu, T. Ono, *Appl. Phys. Lett.* 2007, 90, 162 509-511.
- (18) C.-B. Rong, D. Li, V. Nandwana, N. Poudyal, Y. Ding, Z. L. Wang, H. Zeng, J. P. Liu, *Adv. Mater.* 2006, 18, 2984-2988.
- (19) M. J. Kramer, R. W. McCallum, I. A. Anderson, S. Constantinides, *J. Min. Met. Mat. Soc.* 2012, 64, 752-761.
- (20) N. Poudyal and J. Ping Liu, *J. Phys. D: Appl. Phys.* 2013, 46 043001-043023.
- (21) I. C. Nlebedim, J. E. Snyder, A. J. Moses, D. C. Jiles, *IEEE Trans. Magn.* 2012, 48, 3084-3087.
- (22) X. F. Zhao, Y. C. Zhang, S. L. Xu, X. D. Lei, and F. Z. Zhang, *J. Phys. Chem. C* 2012, 116, 5288-5294.
- (23) L. Enio, E. L. Winkler, D. Tobia, H. E. Troiani, R. D. Zysler, E. Agostinelli, and D. Fiorani, *Chem. Mater.* 2012, 24, 512-516.
- (24) L. Hu, C. D. Montferrand, Y. Lalatonne, L. Motte, and A. Brioude, *J. Phys. Chem. C*, 2012, 116, 4349-4355.
- (25) Q. Song, and Z. J. Zhang, *J. Am. Chem. Soc.*, 2012, 134, 24-28.
- (26) B. H. Liu, J. Ding, Z. L. Dong, C. B. Boothroyd, J. H. Yin, and J. B. Yi, *Phys. Rev. B* 2006, 74, 184427-184436.

- (27) Y. C. Wang, J. Ding, J. B. Yi, B. H. Liu, T. Yu, and Z. X. Shen, *Appl. Phys. Lett.* 2004, 84, 2596-2598.
- (28) R. T. Olsson, S.-A. German, M. S. Hedenqvist, U. W. Gedde, F. Lindberg, and S. J. Savage, *Chem. Mater.* 2005, 17, 5109-5118.
- (29) G. V. M. Jacintho, A. G. Brolo, P. Corio, P. A. Z. Suarez, J. C. Rubim, *J. Phys. Chem. C* 2009, 113, 7684-7691.
- (30) X. Wang, J. Zhuang, Q. Peng, Y. D. Li, *Nature* 2005, 437, 121-124.
- (31) M. Sorescu, A. Grabias, D. Tarabasanu-Mihaila, L. Diamandescu, *J. Appl. Phys.* 2002, 91, 8135-8139.
- (32) Y. S. Yu, A. Mendoza-Garcia, B. Ning, S. H. Sun, *Adv. Mater.* 2013, 22, 3090-3094.
- (33) D. Kim, N. Lee, M. Park, B. H. Kim, K. An and T. Hyeon, *J. Am. Chem. Soc.*, 2009, 131, 454-455.
- (34) H. Yang, T. Ogawa, D. Hasegawa, and M. Takahashi, *J. Appl. Phys.* 2008, 103, 07D526-07D528
- (35) L. Wang, and L. Gao, *J. Phys. Chem. C* 2009, 113, 15914-15920
- (36) M. V. Kovalenko, M. I. Bodnarchuk, R. T. Lechner, G. Hesser, F. Schäffler, and W. Heiss, *J. Am. Chem. Soc.*, 2007, 129, 6352-6353
- (37) A. P. LaGrow, B. Ingham, S. Cheong, G. V. M. Williams, C. Dotzler, M. F. Toney, D. A. Jefferson, E. C. Corbos, P. T. Bishop, J. Cookson, and R. D. Tilley, *J. Am. Chem. Soc.*, 2012, 134, 855-858
- (38) M. Chen, J. Kim, J. P. Liu, H. Fan, and S. H. Sun, *J. Am. Chem. Soc.*, 2006, 128, 7132-7133
- (39) J. Zhang, and J. Fang, *J. Am. Chem. Soc.*, 2009, 131, 18543-18547
- (40) B. P. Pichon, O. Gerber, C. Lefevre, I. Florea, S. Fleutot, W. Baaziz, M. Pauly, M. Ohlmann, C. Ulhaq, O. Ersen, V. Pierron-Bohnes, P. Panissod, M. Drillon, and S. Begin-Colin, *Chem. Mater.*, 2011, 23, 2886-2900
- (41) H. Zeng, P. M. Rice, S. X. Wang, and S. H. Sun, *J. Am. Chem. Soc.*, 2004, 126, 11458-11459
- (42) S. H. Sun, H. Zeng, D. B. Robinson, S. Raoux, P. M. Rice, S. X. Wang, and G. Li, *J. Am. Chem. Soc.*, 2004, 126, 273-279
- (43) S. G. Kwon, Y. Piao, J. Park, S. Angappane, Y. Jo, N.-M. Hwang, J.-G. Park, and T. Hyeon, *J. Am. Chem. Soc.*, 2007, 129, 12571-12584
- (44) K. Maaz, A. Mumtaz, S.K. Hasanain, A. Ceylan, *J. Magn. Mater.* 2007, 308, 289-295
- (45) C. N. Chinnasamy, M. Senoue, B. Jeyadevan, O. Perales-Perez, K. Shinoda, and K. Tohji, *J. Colloid Interface Sci.* 2003, 263, 80-83